

Challenges for Polarimetry at the ILC

Moritz Beckmann, Anthony Hartin, Jenny List

DESY - FLC

EUCARD Workshop
“Spin optimization at Lepton accelerators”

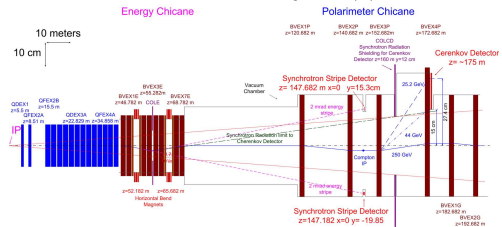
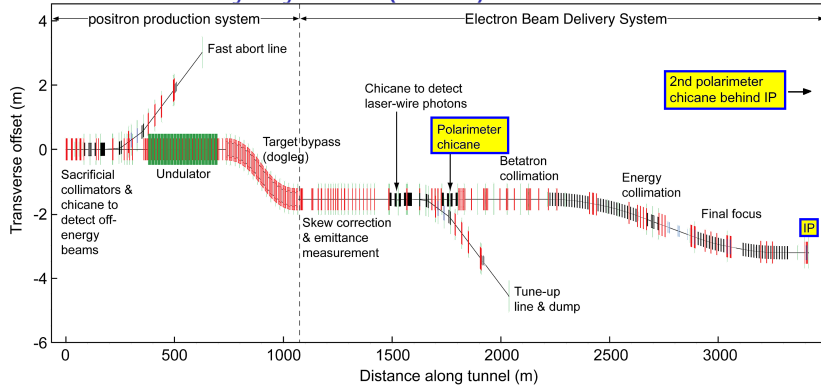
Mainz, Germany
February 12, 2014



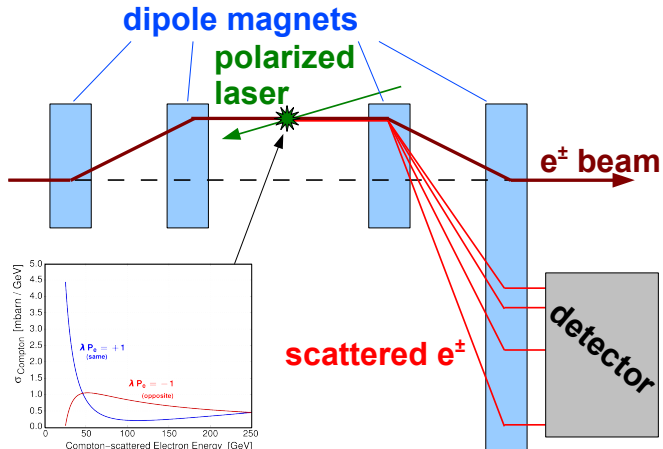
Outline

- Introduction
 - Polarimetry in the ILC beam delivery system
 - Spin transport
- Results
 - Beamline simulation
 - Collision effects
 - Polarization measurement at the disrupted beam
 - Beamline design in view of the polarization measurement
 - Impact of the laser spot size at the downstream polarimeter

ILC Beam Delivery System (BDS)

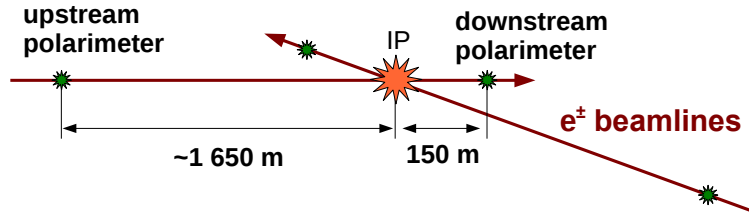


Laser Compton Polarimeter (Principle)



- Laser: **Compton scattering** $e^\pm \gamma \rightarrow e^\pm \gamma$
- Scattering cross section depends on P_z
- Magnet chicane separates scattered e^\pm from beam
- P_z is determined from scattered electrons

Polarimetry at the ILC



- Two Compton polarimeters per beam to measure \mathcal{P}_z
 - Upstream polarimeter undisturbed by collision effects
 - Downstream polarimeter assesses collision effects
 - 0.25 % systematic uncertainty (goal)
- **What do these measurements tell us about the longitudinal polarization at the IP?
→ spin transport simulation**
- Aim to understand spin transport to 0.1 %

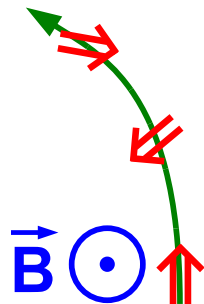
Spin Precession

- Spin precession in electromagnetic fields:
T-BMT equation
- For \vec{B}_\perp only:

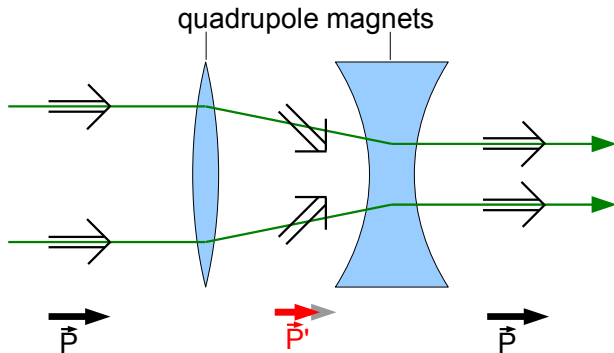
$$\vartheta_{\text{spin}} = \mathbf{b}(\mathbf{E}) \cdot \vartheta_{\text{orbit}}$$

$$b(E) = a\gamma + 1 = \frac{g-2}{2} \cdot \frac{E}{m} + 1 \\ \approx \mathbf{568} \text{ for 250 GeV-electrons}$$

- Dipole magnets, no beam energy spread:
spin vectors precess uniformly, $|\vec{\mathcal{P}}|$ conserved



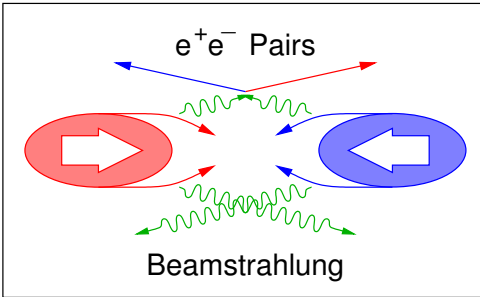
Spin Fan-Out in Quadrupole Magnets



For illustration purposes, the second quadrupole is stronger. Two-dimensional betatron oscillations are not taken into account here.

- Different precession angles after first quadrupole
⇒ polarization $|\vec{P}|$ decreases
- $|\vec{P}|$ recovered by second quadrupole

Beam-Beam Collision Effects

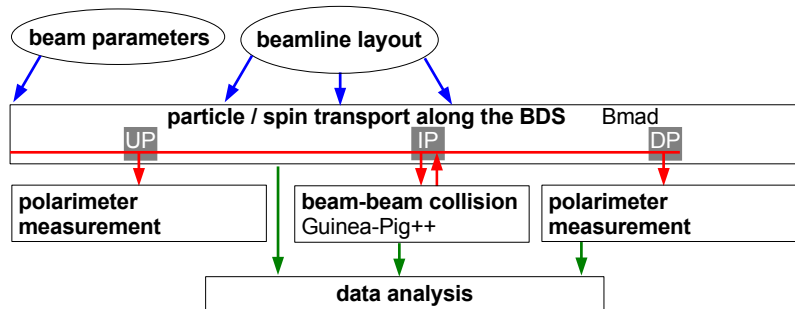


A. Vogel

Bunches focus each other by their electromagnetic fields:

- **Spin fan-out** (like in quadrupole magnets)
- **Spin flip** by emission of **beamstrahlung**
(Sokolov-Ternov effect)

Spin Transport Simulation Framework

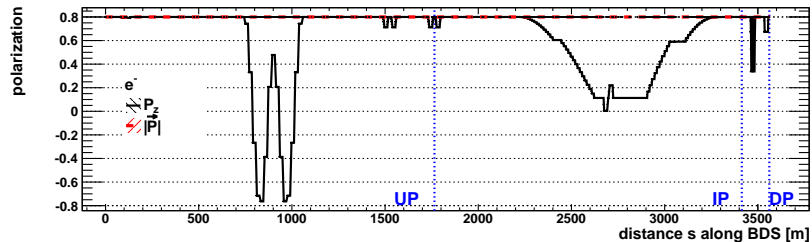
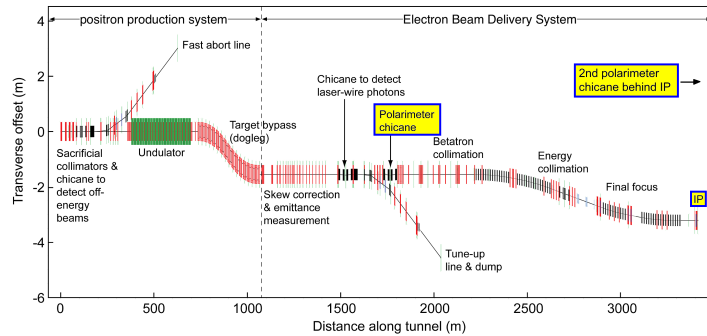


- Developed a beamline simulation (based on Bmad)
- Simulate 40 000 (macro)particles per bunch, generated from beam parameters at the beginning of the BDS
- Interfaced directly to the simulation of the collisions (Guinea-Pig++)

Results

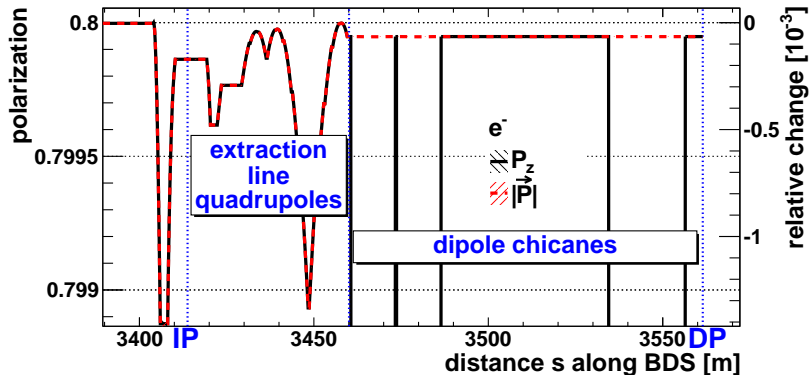
- $\sqrt{s} = 500 \text{ GeV}$
- Beam parameters according to Reference Design Report (RDR, 2007)
- Collision effects also for beam parameters according to Technical Design Report (TDR, 2013)

Spin Transport in the BDS: Basic Configuration



UP/DP: up-/downstream polarimeter

Spin Transport in the BDS: Basic Configuration



DP: downstream-polarimeter

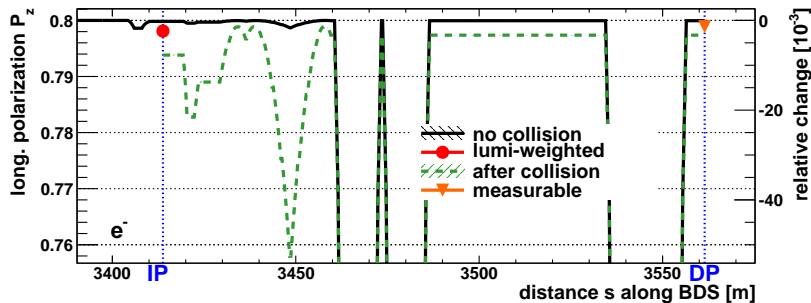
- Quadrupoles cause spin fan-out
- Changes in \mathcal{P}_z well below 0.1 % without collisions

Factors affecting the spin transport (without collisions)

contribution	uncertainty [10^{-3}]
Beam and polarization alignment ($\Delta\vartheta_{\text{bunch}} = 50 \mu\text{rad}$, $\Delta\vartheta_{\text{pol}} = 25 \text{ mrad}$)	0.72
Random misalignments ($10 \mu\text{m}$)	0.43
Variation in beam parameters (few %)	0.03
Bunch rotation (crab cavities)	< 0.01
Detector solenoid	0.01
Synchrotron radiation	0.005
Total (quadratic sum)	0.85

Now: e^+e^- beam collisions

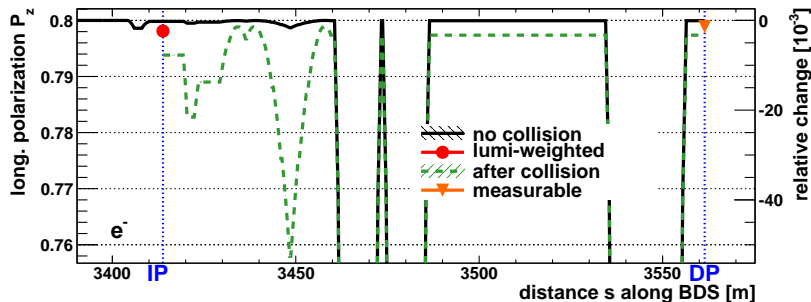
Spin Transport after Collision



DP: downstream-polarimeter

- **Luminosity-weighted (●):** P_z of the colliding particles
- Larger angular divergence / energy spread after collision
- Large spin fan-out in extraction line quadrupoles

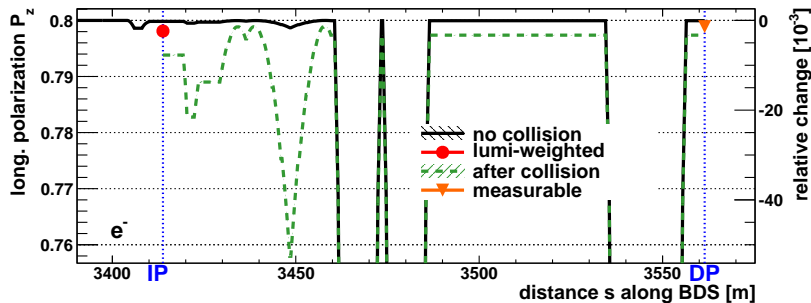
Spin Transport after Collision



DP: downstream-polarimeter

- Extraction line design: restore luminosity-weighted P_z (●) at the downstream polarimeter
- Employ spin fan-out: focus beam at downstream polarimeter with half divergence angle w. r. t. the IP

Spin Transport after Collision



DP: downstream-polarimeter

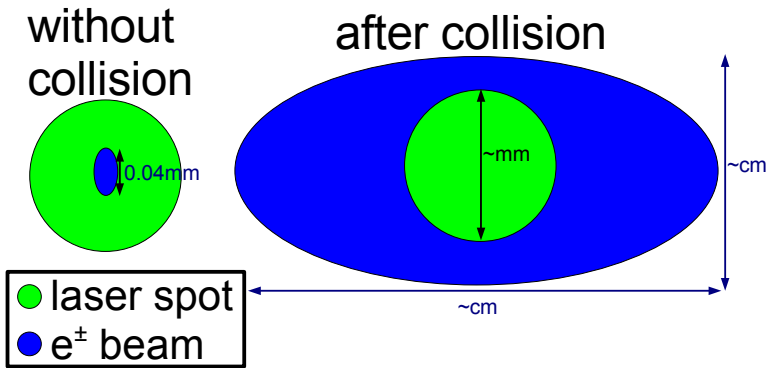
$$\theta_x \gg \theta_y \quad \Rightarrow \quad \Delta P_z \propto \theta_x^2$$

$$\Delta P_z^{\text{lum}} \approx \frac{1}{4} \Delta P_z \propto \left(\frac{\theta_x}{2} \right)^2$$

$$\text{Idea: } |R_{22}(\text{IP} \rightarrow \text{DP})| = 0.5 \quad \Rightarrow \quad P_z^{\text{lum}} = P_z^{\text{DP}}$$

Further reading: SLAC-PUB-4692, SLAC-PUB-8397

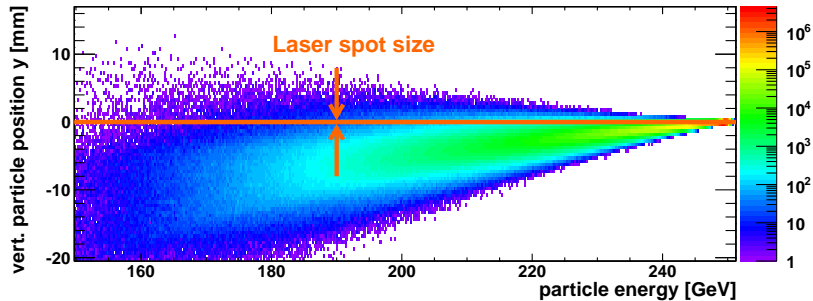
Laser and Particle Bunch at the Downstream Polarimeter



- Without collision: entire beam exposed to laser
- After collision: center of beam exposed to laser
sample of scattered electrons representative?

Downstream Measurement

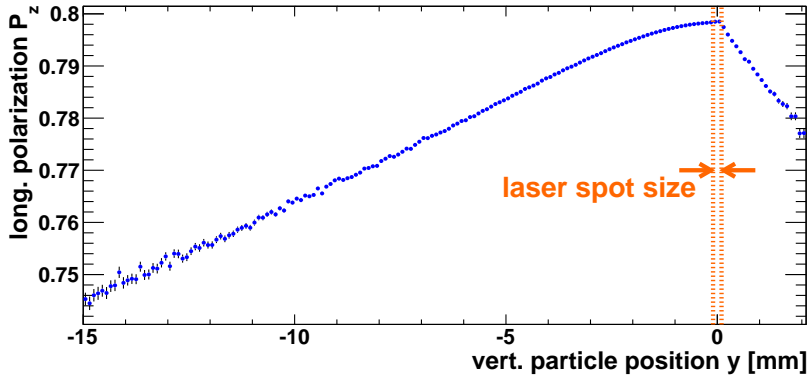
- Downstream polarimeter located in magnet chicane
⇒ particle position correlated with energy (**dispersion**)



- **Laser spot size** at Compton-IP only $\sim 0.1 - 1$ mm

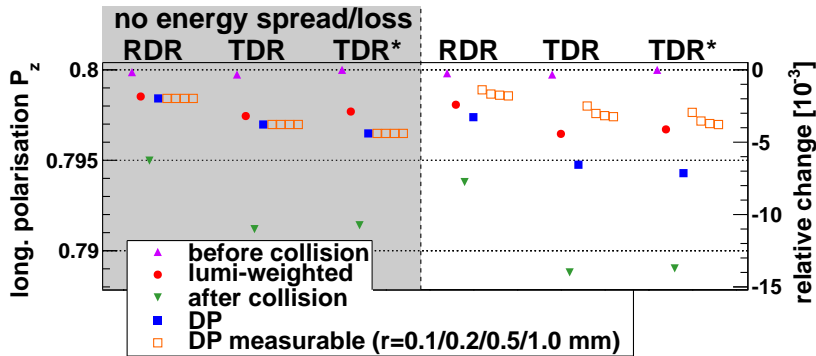
Downstream Measurement

- Beamstrahlung correlates energy and \mathcal{P}_z
⇒ \mathcal{P}_z correlated with particle position
⇒ **Selective measurement, measurement bias**



- *Measurable* longitudinal polarization := average \mathcal{P}_z of particles within a given (laser spot) radius

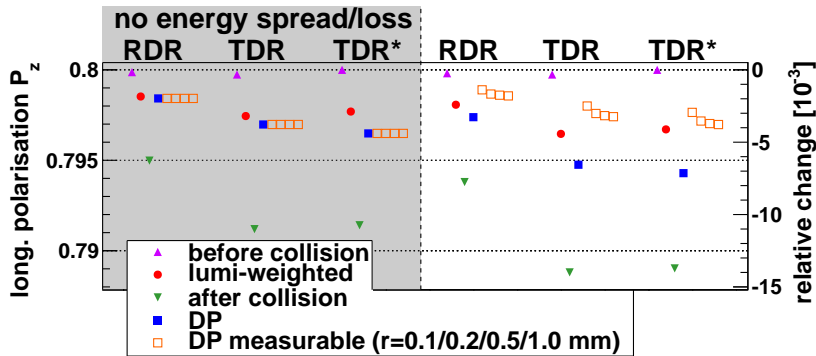
Spin Transport for Different Beam Parameters



DP: downstream polarimeter

- No energy spread/loss: no discrepancy between measurement (\square) and average \mathcal{P}_z (\blacksquare) at downstream polarimeter
- RDR → TDR: stronger focussing \Rightarrow higher collision intensity \Rightarrow larger spin fan-out in collision and afterwards

Spin Transport for Different Beam Parameters

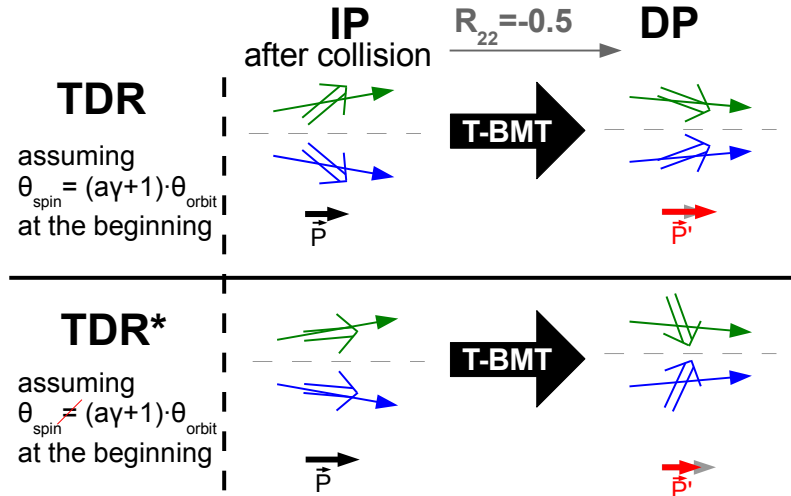


DP: downstream polarimeter

Extraction line design: restore P_z^{lum} (●) at downstream pol. (■)

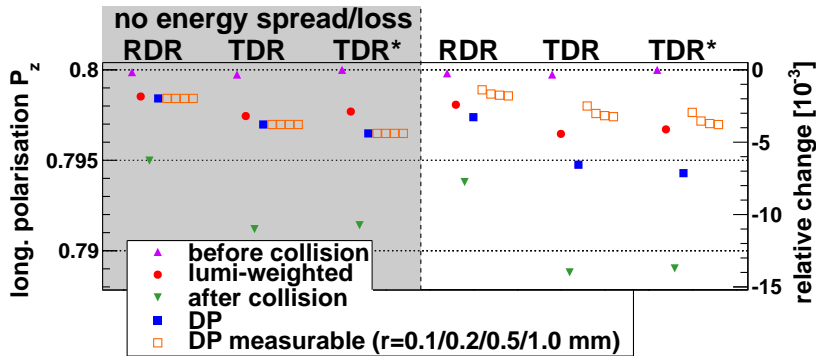
- Design ($|R_{22}| = 0.5$) assumes $D_x \ll 1$
 $D_x^{\text{RDR}} = 0.17$ $D_x^{\text{TDR}} = 0.3$
- More beamstrahlung (not accounted for by design)

Spin Transport for Different Spin Configurations



For illustration only. All angles exaggerated. Beamstrahlung effects neglected.

Spin Transport for Different Spin Configurations

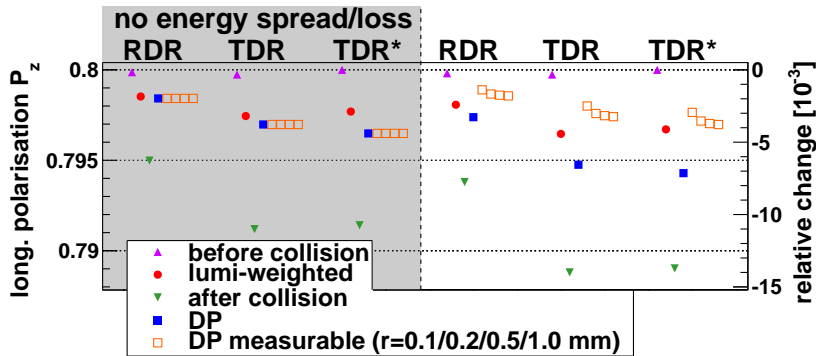


DP: downstream polarimeter

TDR* with respect to TDR:

- All spin vectors parallel before collision, bunch focussed (45 μrad divergence angle)
- Mostly same behaviour in collision (\blacktriangle , \bullet , \blacktriangledown), but different value at downstream polarimeter (\blacksquare)

Spin Transport for Different Beam Parameters



DP: downstream polarimeter

- Polarization varies by several % along the extraction line
- Discrepancies between P_z^{lum} and P_z at the downstream pol. (\bullet , \blacksquare , \square) in the range 0.1 – 0.4 %; discrepancies cancel partially, but only coincidentally

Conclusions

- Cross-calibration (without collisions) to precision of $< 0.1\%$
- Polarization vector alone not sufficient anymore to describe spin configuration of beam:
 - Spin fan-out becomes relevant due to higher measurement precision, higher energy and more intensive collisions
 - How well do we know the initial spin configuration?
→ “cradle-to-grave” simulation
- Extraction line design (restore P_z^{lum} at downstream pol.):
 - Works as foreseen for low-intensity collisions ✓
 - TDR beam parameters: higher intensity → larger discrepancies
 - Beamstrahlung not taken into account; D_x no longer $\ll 1$
 - Disrupted beam lets knowledge of the laser spot size/position at the downstream polarimeter become crucial for the measurement precision
 - Larger laser-spot? Drawbacks: required laser power, low-energy tail undesired in polarimeter

Thanks for your attention!

Further reading:

- DESY-THESIS-13-053
- Publication in preparation

<http://www-library.desy.de/preparch/desy/thesis/desy-thesis-13-053.pdf>

Backup Slides

Differences RDR - TDR

Parameter	symbol	RDR	TDR
Bunches per train		2 625	1 312
Horizontal bunch size	σ_x	[nm]	639
Vertical bunch size	σ_y	[nm]	5.7
Beam energy spread (e^-/e^+)	σ_E/E	$[10^{-3}]$	1.4/1.0
e^+e^- luminosity incl. waist shift	\mathcal{L}	$[10^{38} \text{ m}^{-2} \text{ s}^{-1}]$	2
1.8			
Beamstrahlung parameter	Υ_{global}	0.048	0.062

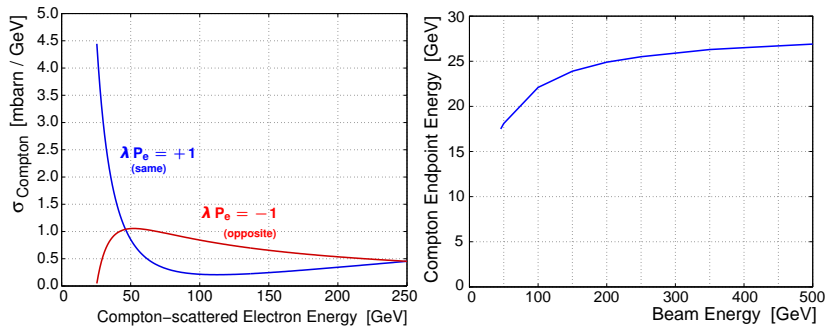
Thomas-Bargmann-Michel-Telegdi (T-BMT) Equation

$$\frac{d}{dt} \vec{S} = (\vec{\Omega}_B + \vec{\Omega}_E) \times \vec{S}$$

$$\begin{aligned}\vec{\Omega}_B &= -\frac{q}{m\gamma} \left((1 + a\gamma) \vec{B} - \frac{a \vec{p} \cdot \vec{B}}{(\gamma + 1) m^2 c^2} \vec{p} \right) \\ &= -\frac{q}{m\gamma} \left((1 + a\gamma) \vec{B}_{\perp} + (1 + a) \vec{B}_{\parallel} \right)\end{aligned}$$

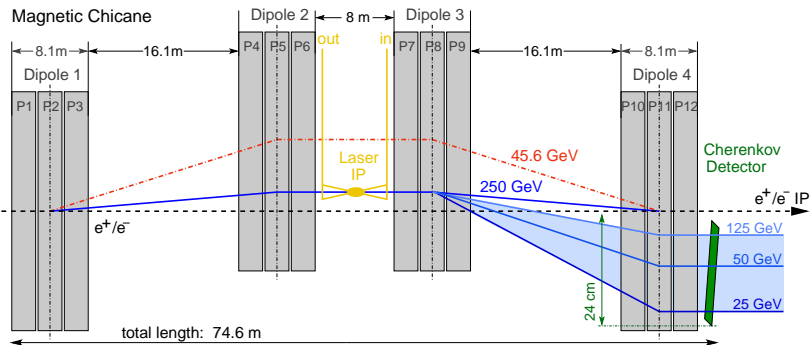
$$\vec{\Omega}_E = \frac{q}{m\gamma} \cdot \frac{1}{mc^2} \left(a + \frac{1}{1 + \gamma} \right) \vec{p} \times \vec{E}$$

Compton Scattering



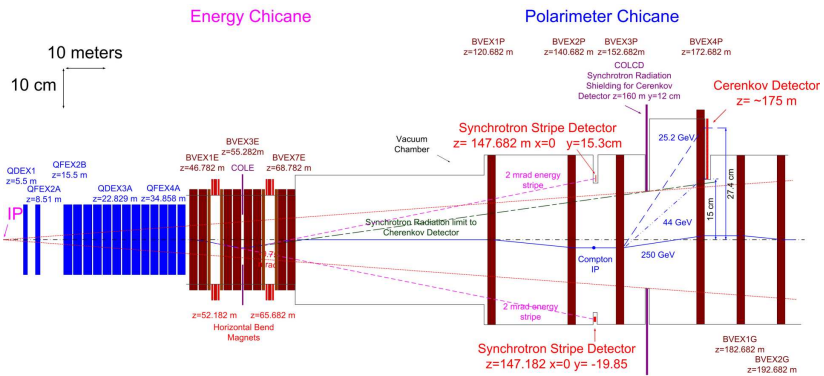
Polarimeter Chicane (upstream)

- Constant magnetic field
- Dispersion (depending on beam energy): 1-11 cm
- Scattering for every bunch per bunch train
- Energy spectrum is polarization-dependent
- Energy distribution → spatial distribution
- Cherenkov gas detector counts electrons per channel

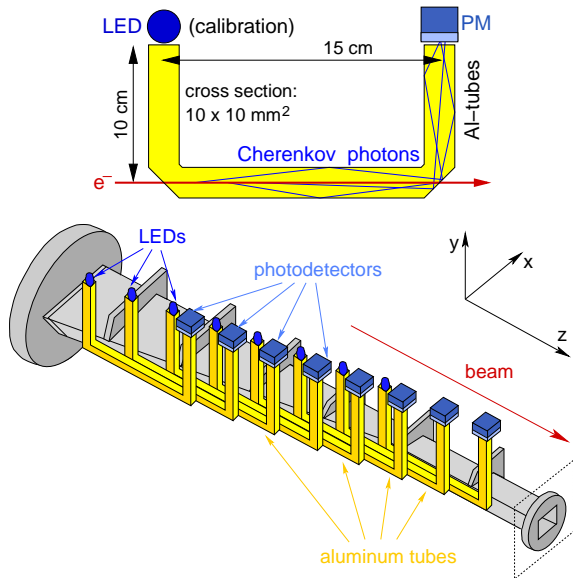


Polarimeter Chicane (downstream)

- Constant magnetic field
- Dispersion (depending on beam energy): 1-11 cm
- Scattering for 3 bunches per bunch train
- Energy spectrum is polarization-dependent
- Energy distribution → spatial distribution
- Cherenkov gas detector counts electrons per channel



Polarimeter Detector

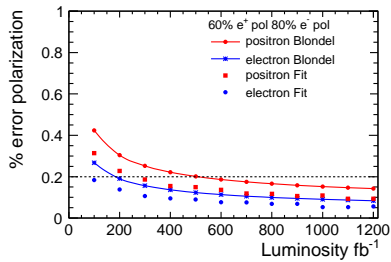
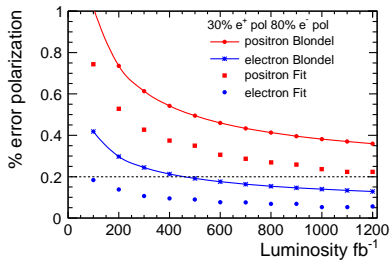


Compton Polarimeters: Systematic Errors

Goal: relative systematic error on measurement < 0.25 %
(SLD polarimeter: 0.5 %)

- Detector linearity: contribution of $\sim 0.1 - 0.2\%$ (goal)
- Laser polarization: $\sim 0.1\%$ ✓
- Analyzing power: $\sim 0.1\%$ (UP: ✓, DP: ?)
 - Detector alignment: can be determined from data (✓)
0.5 mm precision sufficient
 - Alignment of magnets negligible compared to detector ✓
Field inhomogeneities? to be investigated
 - Disrupted electron beam at downstream polarimeter:
 - Dependence on laser-spot size and position: ??
 - Beam energy spread no concern for small laser-spot sizes
thanks to dispersion ✓

Polarization Measurement at the IP

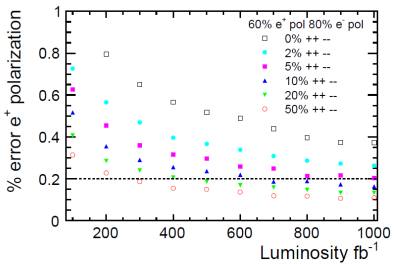
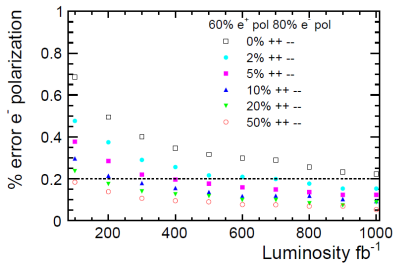


I. Marchesini

Blondel scheme:

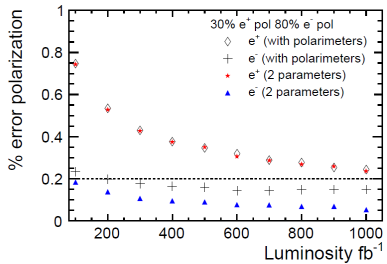
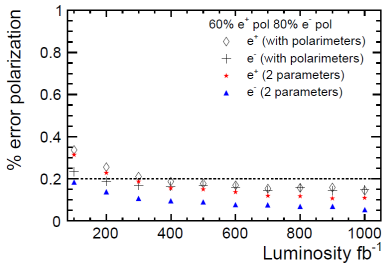
$$|\mathcal{P}_z^{\text{lumi}}(e^\pm)| = \sqrt{\frac{(\sigma_{-+} + \sigma_{+-} - \sigma_{--} - \sigma_{++})(\pm\sigma_{-+} \mp \sigma_{+-} + \sigma_{--} - \sigma_{++})}{(\sigma_{-+} + \sigma_{+-} + \sigma_{--} + \sigma_{++})(\pm\sigma_{-+} \mp \sigma_{+-} - \sigma_{--} + \sigma_{++})}}$$

Polarization Measurement at the IP



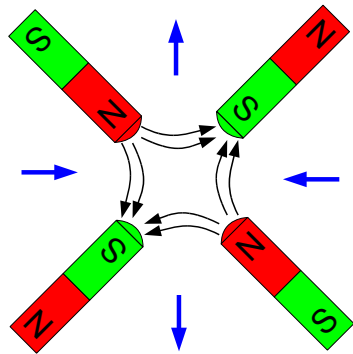
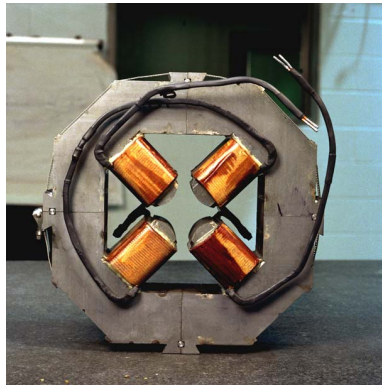
I. Marchesini

Polarization Measurement at the IP



I. Marchesini

Quadrupole Magnet

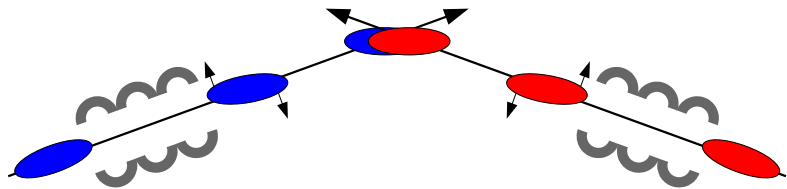


Black arrows: magnetic field lines

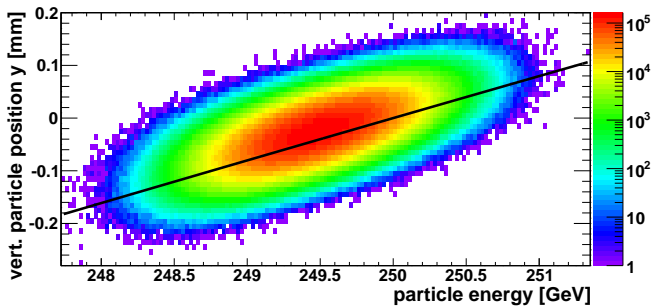
Blue arrows: forces on an incoming electron beam

Bunch Rotation at the IP

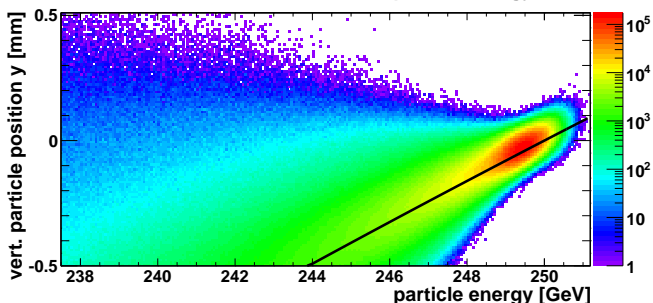
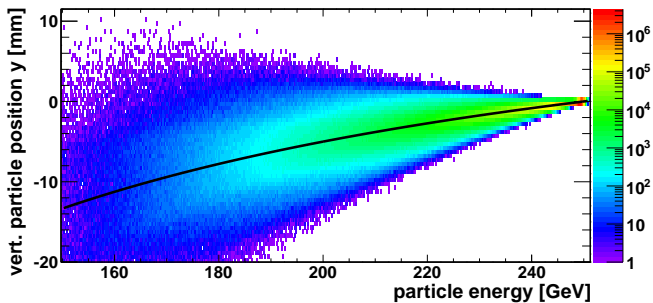
- Collision under crossing angle of 14 mrad
- Maximize luminosity: rotate bunches using *crab cavities*
- Time-dependent transverse deflection of particles



Downstream Pol.: Dispersion w/o Collision

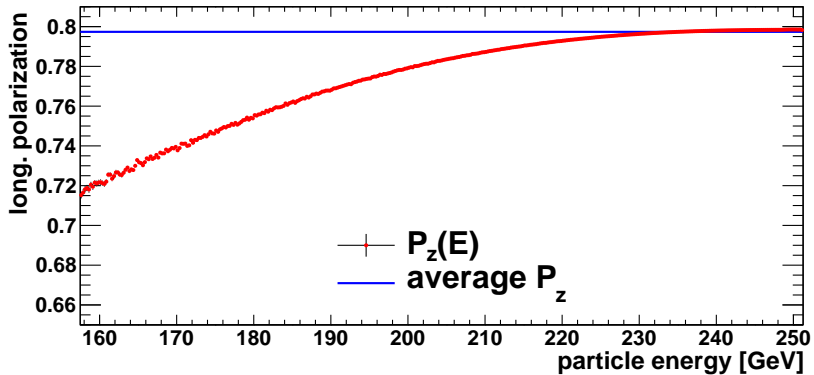


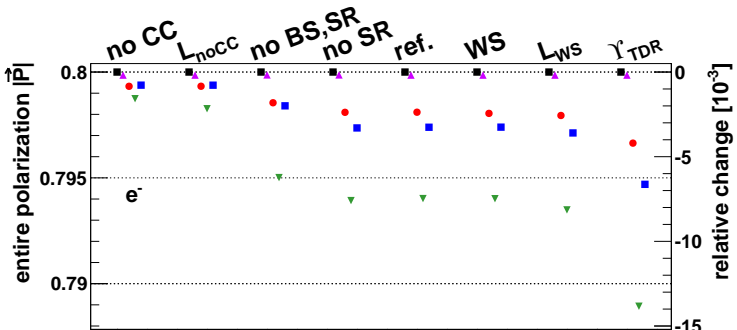
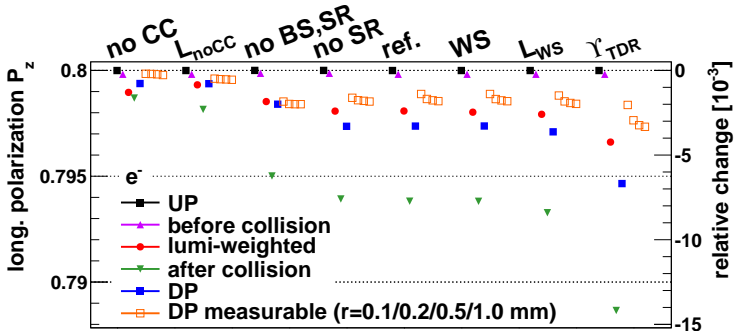
Downstream Pol.: Dispersion after Collision

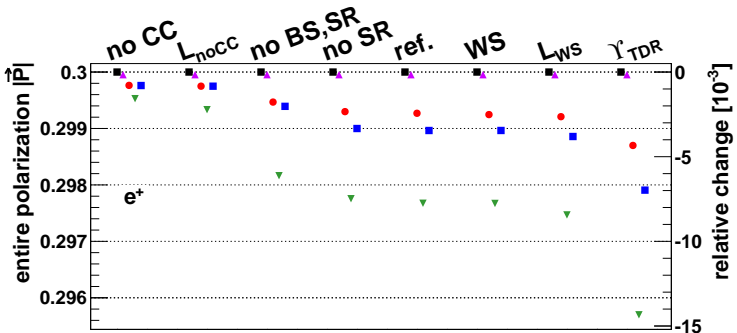
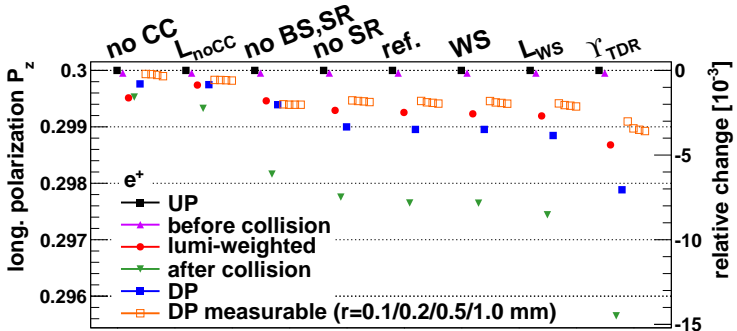


Downstream Measurement

Longitudinal polarization vs. energy at the downstream polarimeter, after collision

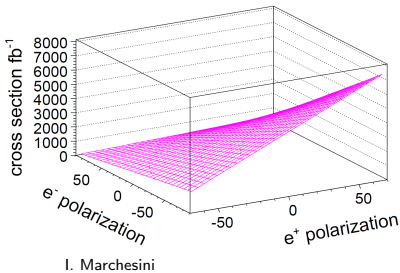
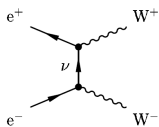






Why Polarization?

Electroweak processes: cross sections depend on \mathcal{P}_z
e. g. $W^+ W^-$ pair production



Polarized beams

- provide new observables
- can be used to enhance/suppress processes

The International Linear Collider (ILC)

- e^+e^- collider as complement to LHC
- $\sqrt{s} \leq 500$ GeV, upgradable to 1 TeV
- Longitudinally polarized beams: $|\mathcal{P}_z(e^-)| = 80\%$
 $|\mathcal{P}_z(e^+)| = 30$ to 60%

